JOURNAL OF APPLIED ELECTROCHEMISTRY 1 (1971) 219–230

Residence time distributions and reaction kinetics in a fuel cell anode

M. DUDUKOVIĆ, H. WEINSTEIN, D. Y. C. NG*

Department of Chemical Engineering, Illinois Institute of Technology, Chicago, Illinois, U.S.A.

Received 22 March 1971

A method which treats the fuel cell anode as a chemical reactor is developed to predict fuel cell performance. The method is based on experimentally measured residence time distribution parameters and differential cell kinetic data. The apparatus and experimental technique used to obtain the gas-phase residence time distributions are described. Kinetic data obtained from differential cell tests of the electrodes are used to evaluate an empirical rate expression.

Axial dispersion model solutions for flow with volume change are obtained, based on the measured Peclet numbers and empirical rate expressions, and compared with experimental data from operating large high-temperature molten carbonate fuel cells. Agreement between the model and the experimentally determined data is very good, but only for low conversions of the fuel.

Introduction

The design of an operable fuel cell is a complex problem. Some of the many aspects of this problem that have to be solved are the electrochemical reaction, adsorption effects on the electrode surfaces, and transport phenomena occurring in the electrolyte. Because of the heterogeneous nature of electrode processes, their kinetics are profoundly affected by the double-layer structure and by adsorption of reactants, products, and supporting electrolyte. Although a lot of work has been done in the past several years in an attempt to understand the fundamental phenomena governing fuel cell performance [1–6, 17, 21] neither a reliable engineering design method nor a scale-up procedure is generally available. The half-cell studies and the experiments with complete cells were mainly designed to determine the overall reaction, its mechanism and order, the role of electrosorption, effects of polarization, and the lifetime of the cells, and to help in the selection between competing electrode materials. There were only a few attempts to treat a fuel cell as a catalytic chemical reactor and to develop design procedures [13, 18].

The object of this work is to obtain an engineering model for fuel cell design. No pretensions are made about clarifying and explaining the basic phenomena governing the electrochemical reaction and its mechanism. An attempt is made to show the various experimental data necessary to obtain an empirical rate expression and predict the performance of a large fuel cell. The methods of chemical reactor design are applied to the fuel cell, and although the electrochemical reaction implies new problems, it is shown that this approach can be used.

These procedures of chemical reactor design rely on residence time distribution measurements taken on the prototype of the full-scale reactor and differential cell kinetic data [13]. The differential rate data required are current density versus concentration curves with terminal voltage as a parameter. An empirically evaluated rate expression can be used with the experimentally determined flow pattern in a large cell to predict its performance. Reaction kinetics and rate expressions based on experimentally proved mechanisms for most of the fuel cell processes remain unknown [1, 3, 4, 17,

* Institute of Gas Technology, Chicago, Illinois, U.S.A.

21] and the geometry of the anode and cathode spaces makes any exact mathematical treatment of the flow very difficult.

As a reaction occurs on the electrode surface it is desirable to attain good transverse mixing in the anode and cathode spaces. High fuel and oxidant flow rates would lead to this goal but these have an undesirable effect on conversion. Low flow rates are usually used. Baffling is introduced to break the parabolic velocity profile and induce vortices and secondary flows. Therefore one cannot consider the flow to be either a fully developed laminar or a perfect plug flow one, and its interpretation through the axial dispersion model appears natural. Good transverse mixing and essentially plug flow is the flow pattern desired in an optimal cell. However, some axial dispersion will most likely be present. With good transverse mixing, one can assume that the reactant is always at the electrode surface in its bulk concentration, which makes the surface reaction equivalent to a homogeneous reaction taking place in the bulk of the fluid. For calculation purposes the reaction per unit of electrode surface can be treated as the disappearance of reactant per unit volume.

The method presented here is an attempt to predict the performance of the large cells on an empirical basis and is general in nature. The high-temperature molten carbonate fuel cell was chosen as an example to demonstrate the method. This cell remains a favoured prospect in fulfilling the ultimate aim of fuel cell development, i.e., in obtaining a system of acceptable capital cost that can operate in an economical manner on low-cost fuels. Only the anode was considered, but a perfectly parallel treatment could be applied to the cathode.

Dispersion model applied to the fuel cell anode

The treatment of the anode was based on the following facts and assumptions.

(i) The overall reaction occurring in the anode is

$$H_2 + CO_3^{2-} \rightarrow H_2O + CO_2 + 2e \quad (1)$$

and the water-gas shift reaction is assumed at equilibrium

$$H_2 + CO_2 \rightleftarrows H_2O + CO. \quad (2)$$

(ii) The empirically obtained rates from differential cell data are assumed to represent point rates within the anode.

(iii) Constant pressure (a negligible pressure drop along the anode was determined experimentally) and temperature of 700°C are maintained in the anode space.

(iv) The whole anode is at a uniform operating (terminal) voltage.

The anode is visualized as a channel of length L and rectangular cross-sectional area A. The equivalent diameter is $4{\cdot}6\times10^{-3}$ m, and the fluid is assumed to be perfectly mixed at any cross-section perpendicular to flow. Because the reactant is available at the electrode surface in its bulk concentration, a reaction taking place at the surface can be considered as the disappearance of reactant and appearance of product per equivalent volume. The mixing processes in the anode are lumped into the experimentally determined dispersion coefficient.

Material balance on hydrogen around an element of the anode yields

$$\frac{d}{dZ}(UC) = \frac{d}{dZ}\left(D\frac{dC}{dZ}\right) + r. \quad (3)$$

As shown in the following section the empirical rate is obtained from differential cell data in terms of current density which is equivalent to a surface reaction rate

$$J = k_1 y_{H_2}^{1/4}. \quad (4)$$

Then the rate per unit volume is

$$-r = \frac{k_1\times10^{-3}S_e}{C_T^{1/4}n_eFV_a}C^{1/4} = kC^{1/4}. \quad (5)$$

If we neglect the volume change due to reaction in the anode and take D = const, which is the usual assumption in the dispersion model, we get the dispersion equation in the form.

$$D\frac{d^2C}{dZ^2} - U\frac{dC}{dZ} - kC^{1/4} = 0. \quad (6)$$

This generalized equation was solved analytically for the first-order reaction with appropriate boundary conditions by Danckwerts [9] and numerically by Fan and Bailie [12] for the orders of 2, 1/4, 1/2.

The boundary conditions are the following,

discussed in detail by Wehner and Wilhelm [23] and Van der Laan [22]:

$$\left.\begin{aligned} UC - D\frac{dC}{dZ} &= UC_0 \quad Z = 0 \\ \frac{dC}{dZ} &= 0 \qquad\qquad Z = L \end{aligned}\right\} \tag{7}$$

Putting the equation in dimensionless form we get:

$$\frac{d^2c}{dz^2} - \frac{1}{N}\frac{dc}{dz} - \frac{k'}{N}\tau c^{1/4} = 0. \tag{8}$$

Changing the independent variable,

$$1 - z = t \tag{9}$$

we finally obtain an equation and boundary conditions which are easily solved on the analog computer.

$$\frac{d^2c}{dt^2} + \frac{1}{N}\frac{dc}{dt} - \frac{k'}{N}\tau\, c^{1/4} = 0 \tag{10}$$

$$\left.\begin{aligned} &\frac{dc}{dt}(0) = 0 \\ &c(1) + N\frac{dc}{dt}(1) = 1 \end{aligned}\right\} \tag{11}$$

Since there is a net increase in the number of moles during the reaction while total concentration remains constant due to constant pressure and temperature, velocity cannot be considered constant along the channel. Assuming ideal gas behaviour, velocity at any point in the channel is given by:

$$U = U_0(1 + \varepsilon x) \tag{12}$$

where ε is the coefficient of expansion due to reaction and x is the degree of conversion of hydrogen. We have to assume that the axial dispersion coefficient, D, remains constant along the channel, as it is not possible to find its functional dependence on velocity.

If we use the rate expression given by Equation 5 and put Equations 3 and 7 into dimensionless form we get:

$$N\frac{d^2c}{dz^2} - \frac{d}{dz}(uc) - \tau k'c^{1/4} = 0 \tag{13}$$

and

$$u = \frac{1 + \varepsilon}{1 + \varepsilon c} \tag{14}$$

where

$$k' = \frac{k}{C_0^{3/4}} = \frac{k_1 \times 10^{-3} \cdot S_e}{C_T^{1/4} C_0^{3/4} n_e F V_a} \tag{15}$$

and

$$N = \frac{D}{U_0 L}. \tag{16}$$

Using the same change of variable (Equation 9) we get:

$$\frac{d^2c}{dt^2} + \frac{1 + \varepsilon}{N(1 + \varepsilon \cdot c)^2}\frac{dc}{dt} - \frac{\tau k'}{N}c^{1/4} = 0 \tag{17}$$

with boundary conditions given by Equation 11.

Equations 10 and 17 are very suitable for integration on the analog computer and solutions were obtained in this manner. The concentration profiles along the reactor length were obtained for several different values of the parameters. The dimensionless concentration at $t = 0$, which corresponds to $z = 1$, at the vessel exit is used to calculate final conversion from the relationship:

$$x = \frac{1 - c}{1 + \varepsilon c}. \tag{18}$$

With flow rate, final conversion, and operating voltage known, the current and power withdrawn from the cell can be found using Faraday's law.

Evaluation of kinetic data

Work on high-temperature fuel cells has been going on since the early experiments of Baur [2] in 1921 and Davytan [10] in 1946. The operation of fuel cells at high temperature using molten carbonate electrolytes has two main advantages. First, problems of overpotential losses at the electrodes are considerably reduced at high temperature. Second, the problem of CO_2 rejection is circumvented by using molten carbonates. In the last decade extensive studies on these cells have taken place, especially in Holland and the U.S. The works of Broers [6, 7], Chambers [8], Tantram [21], and Baker [1]

present experimental descriptions of the behaviour of such cells. An optimal electrode material has been chosen [1, 6] (fibre nickel anode and silver cathode) and different mixtures of electrolytes employed [1, 4–7, 16, 21, 24]. The mechanism of the reaction and its rate-determining step still remain unknown [1, 3, 5, 6]. Although there is no general agreement on whether the fuel oxidation in the anode is of primary or secondary nature, some claims have been made that the cell should be considered as a concentration cell in which primary anodic and cathodic processes are the same [8, 21]. Others proved that a concentration cell approach is not likely to be correct [4, 5].

It has been agreed upon that the purely resistive *IR* drop is always the predominant term in the total voltage drop of a current-delivering cell [1, 6]. Electrode polarization, though, is not negligible, especially at higher conversions, and is due to mass transport phenomena or to activation-controlled processes. It is felt that the observed polarization is due to the change in surface concentrations necessary to produce the diffusion rates of reactants and products to meet the requirements of the processes occurring [21]. Definite experimental evidence on these questions has not yet been obtained. Data available in the literature [1, 3, 5–8, 21] present the well-known terminal voltage-current density curves.

A complete description of the performance of a cell requires a set of voltage-current density curves at different levels of gas consumption [8]. Such curves of anode and cathode potentials (*IR*-free with Pt electrode as the reference) versus current density have been obtained at certain levels of fuel and oxidant consumption [1, 6, 7] as have curves of terminal voltage versus fuel conversion with current density as the parameter [1]. All these data were obtained on cells with substantial electrode areas so that the fuel gas changed its composition considerably during its passage through the anode space. It is known that terminal voltage is a function of gas feed rate and current density, i.e., it is dependent on the Nernst potential, current density, and polarization. The Nernst potential, however, is a function of composition and temperature only. When a fuel cell operates at constant temperature, E, the theoretical cell potential changes according to the Nernst equation as the composition changes in either the anode or cathode or both. As a consequence of the change in E that is due to the change in composition, the current density of the cell must vary from point to point. When the cell electrodes have high electronic conductivity, the voltage, V, for the cell has a virtually uniform value over their entire area, and this operating (terminal) voltage is dependent on the exit gas composition [8].

The current withdrawn from the cell is given by

$$I = v \cdot \rho_m \cdot F \cdot n_e x \tag{19}$$

and the average current density, which is recorded from all the large cells, is:

$$J = \frac{I}{S_e}. \tag{20}$$

Knowing the terminal voltage of the cell and fuel conversion per pass we can predict the cell performance.

It is commonly accepted [1, 3, 5, 6] that the following reactions occur at the electrodes of a high-temperature molten carbonate fuel cell using H_2 as fuel and air as the oxidant.

$$\text{Anode:} \quad H_2 + CO_3^{2-} \rightarrow H_2O + CO_2 + 2e^- \tag{21}$$

$$\text{Cathode:} \quad 1/2\, O_2 + 2e^- + CO_2 \rightarrow CO_3^{2-}. \tag{22}$$

The water-gas shift reaction establishes an equilibrium at the anode

$$CO_2 + H_2 \rightleftarrows CO + H_2O \tag{23}$$

but has practically no influence upon the composition of the anodic outlet according to Broers [7].

The theoretical voltage for the cell is given by the Nernst equation:

$$E = E^\circ - \frac{RT}{2F} \ln \frac{P_{H_2O\,(a)} \cdot P_{CO_2\,(a)}}{P_{H_2\,(a)} \cdot P_{CO_2\,(c)} \cdot P^{\frac{1}{2}}_{O_2(c)}}. \tag{24}$$

Ohmic and concentration polarization are the components of the overvoltage, η, that reduce the theoretical electromotive force to an operating (terminal) voltage:

$$V = E - \eta. \tag{25}$$

It is of interest to obtain the relationship

between current density and gas composition which will yield a desired empirical rate expression equivalent to those used in chemical kinetics. One cannot obtain this information from the large cells as the current density measured there is equivalent to a surface area average of the point rates of reaction. It is desirable to have a cell with very small electrode areas with gas flow rates high enough for the composition to remain practically constant. Keeping the term $P_{CO_2(c)} \cdot P^{\frac{1}{2}}_{O_2\,(c)}$ in the cathode constant and changing the anode ratio $\frac{P_{H_2O\,(a)} \cdot P_{CO_2\,(a)}}{P_{H_2\,(a)}}$ in correct proportions, one could record real point rates at different current densities based on the anode composition only. Such data with the anode ratio kept in correct proportion, to our knowledge were not available. Data obtained in the cells with an electrode area of 3 cm^2 are used in this work [14]. It was possible to assume that the composition of anode and cathode gases does not change per pass, as it was determined experimentally that no increase in current occurred with increased flow rate. Fibre nickel (20% dense) was used for the electrodes while fuel and oxidant flow rates were kept above 1000 cm^3/min. The temperature of operation was maintained at 700°C. Four different gas mixtures were used on the anode side, hydrogen always being the fuel. The compositions of the gases used were

$\%H_2$	$\%CO_2$	$\%N_2$	$\%H_2O$
19	19	57	5
38	19	38	5
57	19	19	5
76	19	0	5

Standard oxidant was used on the cathode side with the following composition: 55% N_2, 30% CO_2, 15% O_2. The results of the tests are presented in the form of electrode voltage (Pt reference) versus current density curves with gas composition as parameter, as shown in Fig. 1 [14].

One can define the empirical reaction order n with respect to hydrogen as

$$n = \left(\frac{\partial \ln J}{\partial \ln C_{H_2}}\right)_{T,\,Ck,\,V} \tag{26}$$

The data from Fig. 1 are plotted as current density, J, versus hydrogen mole fraction, y_{H_2}

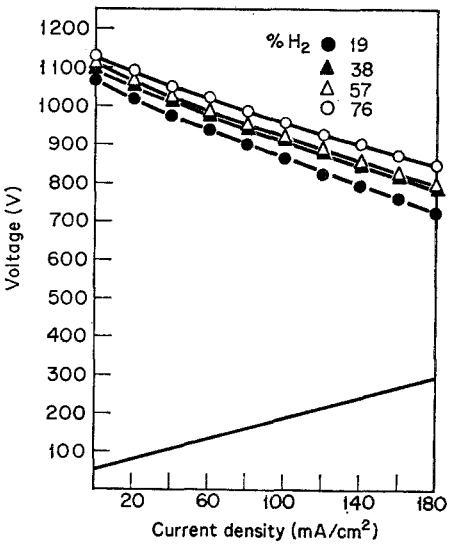

Fig. 1. Differential cell voltage-current density relationship.

on the log-log scale, as shown in Fig. 2. The relationship was found to be of the form

$$J = k_1\, y^n_{H_2} \tag{27}$$

The reaction order with respect to hydrogen, n, was found to be 1/4; the reaction rate constant, k_1, varies with voltage. Such an empirical rate expression is completely analogous to the chemical rate expression where the rate is an n^{th}-order function of concentration and the

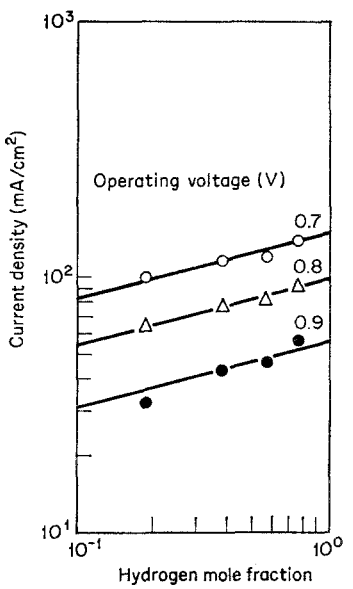

Fig. 2. Log of current density-log of hydrogen mole fraction relationship.

specific rate constant a strong function of temperature or catalyst activity. Here the rate constant appears to be a strong function of the operating voltage. Hence, for engineering purposes such an expression can be used successfully for desired operating voltage in predicting the large-cell performance.

The same electrodes (fibre 20% dense) and electrolyte were used in operating the large cells with 175 cm^2 of electrode area at 700°C. Fuel with a composition of 64% H_2, 16% CO_2 and 20% H_2O was used on the anode side and the same standard oxidant on the cathode side. The flow rates of the fuel were varied from 300 to 1200 cm^3/min, while the oxidant flow rate was much larger, exceeding 3000 cm^3/min and thus implying a nearly constant composition on the cathode side. Therefore, only the anode reactions could be studied.

Experimental procedure for obtaining residence time distributions

The basis for the choice of an axial dispersion model for this analysis is that if the flow in the anode space is turbulent enough that transverse mixing is good. If this is the case, residence time distributions in the anode space should be narrow (small variance) and almost symmetric (small skewness). These conditions are also desirable from the standpoint of optimal design of the fuel cell as noted previously. The design of the anode used in this work is shown in Fig. 3. The path of the fluid is broken by several bends which include contractions and expansions.

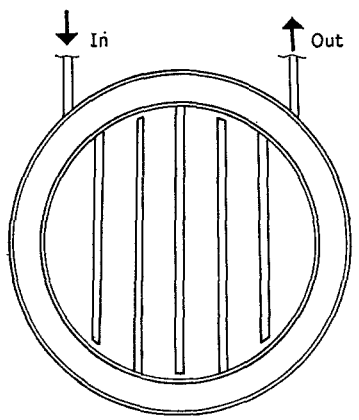

Fig. 3. Schematic diagram of fuel cell anode.

These tend to break up any developing profile and cause secondary flows. Then while the Reynolds number is in the laminar range and the total length-to-diameter ratio of the anode space is large the flow will never attain fully developed profiles of either velocity or concentration.

Since the flow patterns are quite complex, the only method available to determine whether the axial dispersion model is applicable and if so what the dispersion numbers are, is residence time distribution measurements.

Tracer analysis is well developed in chemical engineering [15, 16] but to our knowledge there is no published work available on the residence time distributions of flow in fuel cells.

Information about the flow patterns within the anode of the large cell was obtained by monitoring the response to a pulse input of tracer, $C_m(t)$. As a sampling system had to be used to record gas-phase tracer concentration, the response obtained was the convolution of the response of the anode, $C_a(t)$, and the sampling system distortion, $G_s(t)$ [19]. The nonideality of the pulse can be lumped with the sampling system distortions, $G_s(t)$. The measured response is given by the following convolution integral:

$$C_m(t) = \int_0^t G_s(t-\tau)\, C_a(\tau)\, d\tau \qquad (28)$$

or in the Laplace domain:

$$\bar{C}_M(s) = \bar{G}_s(s) \cdot \bar{C}_a(s). \qquad (29)$$

The response of the sampling system alone, $C_s(t)$, can be measured, $G_s(t)$ evaluated, and deconvolution performed to get the anode response [19] $C_a(t)$:

$$C_s(t) = M_0 \int_0^t G_s(t-\tau)\, \delta(\tau)\, d\tau = M_0 G_s(t)$$

$$G_s(t) = \frac{C_s(t)}{M_0}. \qquad (30)$$

The whole curve of $C_a(t)$ can then be obtained using Fourier transforms. In our case the means and variances of the anode response give sufficient information about the flow patterns of the anode. They can be obtained, using the linear properties of the system, by subtraction of the moments of the sampling system response curve [15, 19]. Linearity of the system is dem-

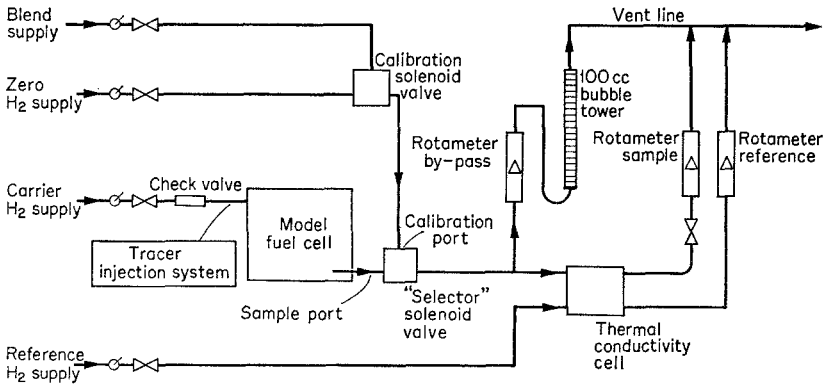

Fig. 4. Schematic apparatus flow diagram.

onstrated by introducing known quantities of tracer, W and $2W$, and observing that the response doubles.

We give here a brief description of the apparatus and experimental technique used for obtaining gas residence time distributions in the large anode. (This is described in detail in Refs. 11 and 20). A pulse injection of CO_2 tracer was made into the hydrogen stream entering the fuel cell anode from a pressurized CO_2 reservoir. Time of injection was about 0·1–0·2 s. Part of the exit stream was passed through a microthermal conductivity cell and the output of that cell recorded as cell voltage versus time. A schematic diagram of the apparatus is given in Fig. 4.

The tracer injection system, Fig. 5, was designed with a twofold purpose; to yield a pulse injection of short enough duration to be mathematically described as the Dirac δ-function and to give an accurate measure of the total tracer injected. To inject tracer, a solenoid valve, normally closed, was momentarily energized by pressing a button, thus allowing the CO_2 tracer to flow from the pressurized reservoir into the carrier-gas stream. The amount of tracer injected was calculated from the reservoir pressure before and after injection, provided the volume of the reservoir was known. This volume was determined experimentally to be 86·5 cm^3 [11].

The microthermal conductivity cell used for concentration measurements had a rapid response of less than 0·2 s, and could detect a tracer concentration as low as 10^{-7} g/l. The output from the cell was directed through an

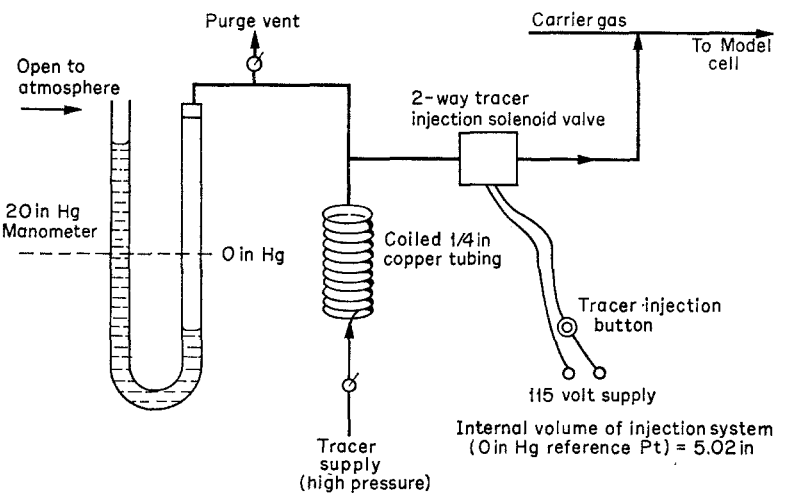

Fig. 5. Tracer injection system.

electric bridge arrangement to a Sargent recorder. The voltage output of the cell is not a linear function of CO_2 concentration, so a calibration run had to be made to transfer the recorded deviation versus time curves to concentration versus time curves.

Experimental runs were performed for seven different flow rates, ranging from 5·8 cm^3/s $\left(348 \frac{cm^3}{min}\right)$ to 35·5 cm^3/s $\left(\frac{2150\ cm^3}{min}\right)$ for the anode plus sampling system and sampling system alone. The above range of flow rates is used in operating the large cells. Examples of the runs are shown in Figs. 6 and 7.

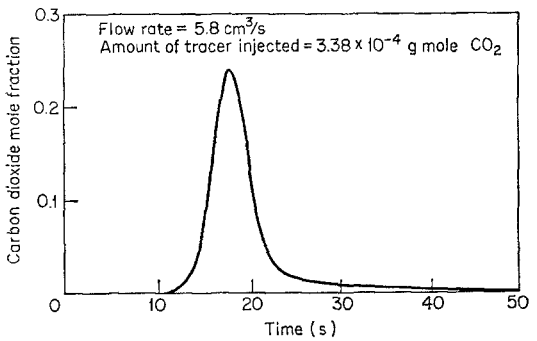

Fig. 6a. Response of anode plus sampling system to an impulse at low flow rate.

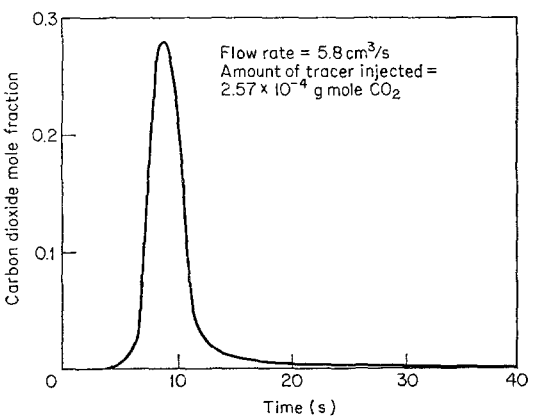

Fig. 6b. Response of sampling system to an impulse at low flow rate.

The response curves show little spread about the peak, which indicates a relatively small deviation from plug flow. Hence the use of the dispersion model is justified. We can assume that the flow in the anode is essentially plug flow

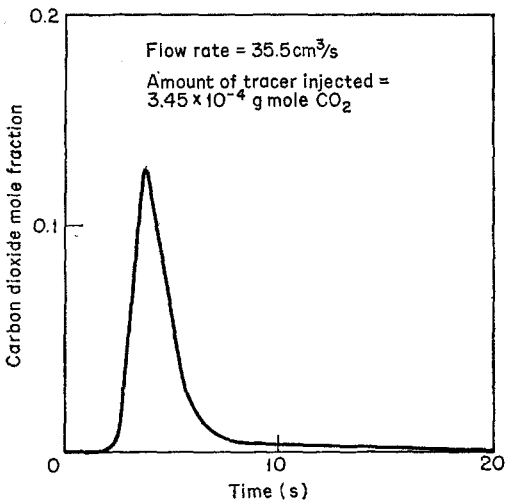

Fig. 7a. Response of anode plus sampling system to an impulse at high flow rate.

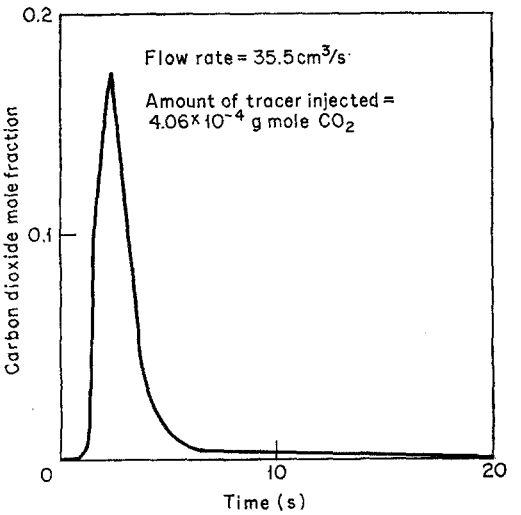

Fig. 7b. Response of sampling system to an impulse at high flow rate.

with some degree of axial dispersion superimposed [15].

The mean, $\bar{t}$, dimensional variance, σ_t^2, and dimensionless variance, σ^2, were calculated for the sampling system and the anode plus sampling system using the following approximate formulae [15].

$$\bar{t} = \frac{\Sigma tC}{\Sigma C} \tag{31}$$

$$\sigma_t^2 = \frac{\Sigma t^2 C}{\Sigma C} - \bar{t}^2 \tag{32}$$

$$\sigma^2 = \frac{\sigma_t^2}{\bar{t}^2}. \tag{33}$$

The mean and variance of the anode itself were calculated by subtraction using the linear properties of the system. The dispersion number, N, which is the inverse of the Peclet number, is obtained through the relationship

$$2N = 2\frac{D}{UL} = \sigma^2 = \frac{2}{Pe}. \tag{34}$$

The mean, variance, apparent anode volume, dispersion number, and intensity of dispersion are presented in Table 1. No dead space is detectable in the range of flow rates used, and the mean value for the anode volume was found to be 55·65 cm^3. The dispersion number range of 0·0575–0·1055 is inconsistent with laminar flow in the anode and justifies the assumption of the axial dispersion model for a system with surface reaction.

It was not possible within these flow variations to find a reasonable trend in dispersion number values, so the dispersion number can be considered fairly independent of the Reynolds number over the range considered.

The intensity of dispersion, $\frac{D}{Ud_e}$, is plotted versus Reynolds number on a logarithmic scale in Fig. 8. The seven experimental points are not sufficient to evaluate a single curve with confidence, but a trend similar to that obtained by Bischoff and Levenspiel for the flow of gases in pipes is apparent [16].

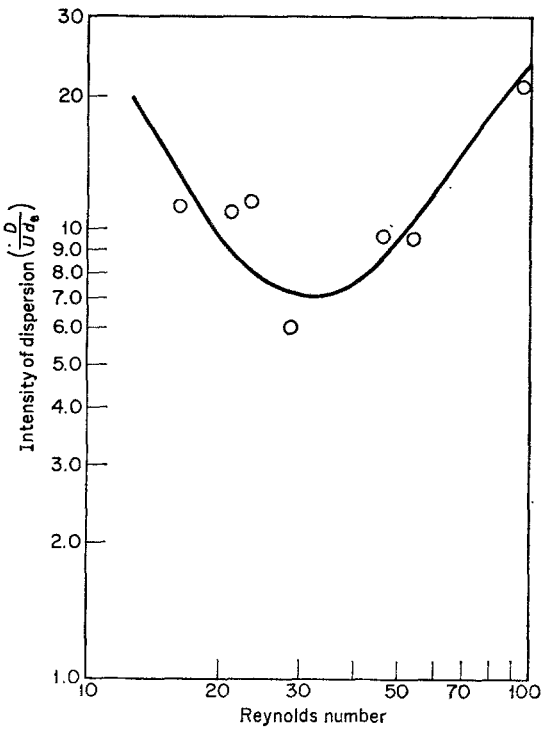

Fig. 8. Intensity of dispersion as a function of Reynolds number.

Results and discussion

The results obtained on the basis of the axial dispersion model with and without volume change are presented in Fig. 9 as conversion versus flow rate calculated for three different values of the operating voltages. It is obvious that conversion decreases with increasing flow rate for constant operating voltage. Conversion decreases with increasing operating voltage for

Table 1. Mean Residence times, variances, dispersion numbers

Run	*Flow rates* cm^3/s	*Mean* $\bar{t}$, *s*	*Volume,* cm^3	σ_t	σ^2	$N=\frac{D}{UL}$	$\frac{D}{Ud_4}$	*Re*
1	5·8	9·9	57·3	11·23	0·115	0·0575	11·20	16·2
2	7·7	7·1	54·6	5·73	0·114	0·0570	11·10	21·6
3	8·3	6·7	55·6	5·45	0·121	0·0605	11·80	23·3
4	10·3	5·0	51·5	1·51	0·061	0·0305	5·95	28·8
5	16·6	3·4	56·5	1·23	0·107	0·0504	9·81	46·5
6	20·0	2·8	56·0	0·79	0·101	0·0501	9·78	56·0
7	35·5	1·6	56·8	0·54	0·211	0·1055	20·58	99·5

average values:
$\bar{V}=55{\cdot}65$ cm^3; $\bar{N}=0{\cdot}0545$

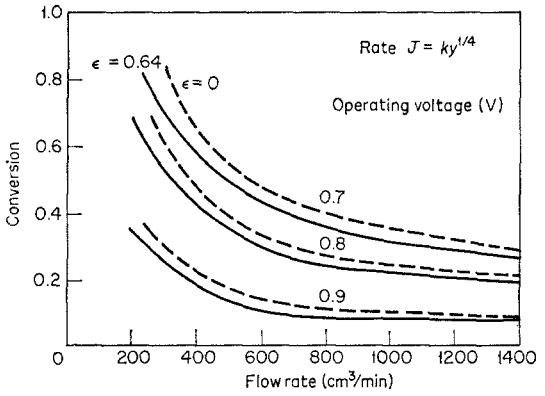

Fig. 9. Final conversion as a function of flow rate.

constant flow rate. This result is also expected as the rate decreases with increasing voltage.

It is seen from Fig. 9 that the increase in number of moles due to reaction has the effect of lowering the conversion, especially at higher rates (low operating voltage) and high conversions (low fuel flow rates).

Fig. 10 compares the results predicted using

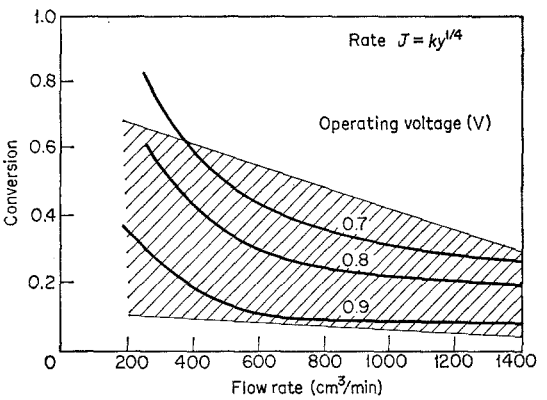

Fig. 10. Computed solutions compared with real data.

Equation 4 for the rate expression in the dispersion model with a broad range of actual data taken in large operating fuel cells [14]. The predicted conversions are higher than the actual data for high values of the reaction rate or low operating voltages and match the data fairly well at low values of the reaction rate or high operating voltages. Unfortunately, a complete description of the conversion data for large cells is not available and some of the curves of current density versus voltage lack information on fuel flow rate. The data are also scattered as different anode designs and various electrodes and electrolytes were used. The differential cell kinetic data used in the analysis are only representative of some of the large-cell data. Many of these large-cell data do not contain information on fuel flow rate and so cannot be used for comparison with our solutions.

Fig. 11 presents predicted values of conversion

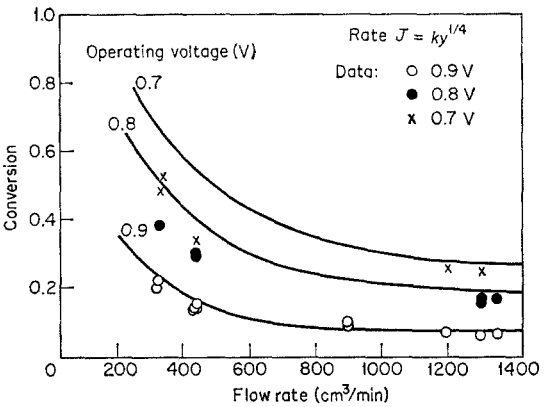

Fig. 11. Computed solutions compared with real data.

compared to a consistent set of experimental data for a set of operating voltages. Total current of the large cell was measured at different fuel flow rates with the voltage within 10% of the desired value.

Very good agreement is obtained at 0·9 V operating voltage over the whole range of flow rates. At a high flow rate of 1300 cm^3/min of fuel, good agreement is also obtained at 0·7 and 0·8 V operating voltage. This indicates that whenever the degree of conversion of hydrogen is low, the empirical rate expression obtained from the differential cell data based only on hydrogen concentration is suitable. However, at higher conversions the products do influence the rate and should be taken into account. Empirical rate expressions from differential cells should be obtained which take into account the effects of product concentration. These results agree with the predictions of Broers [7] that the product accumulation on the electrode surface becomes rate controlling at higher conversions.

Acknowledgment

The Institute of Gas Technology is gratefully

acknowledged for supplying partial support of this work.

Notation

A	cross-sectional area, cm^2
C	concentration of hydrogen, $\left(\frac{\text{g mole}}{cm^3}\right)$
$c = \frac{C}{C_o}$	dimensionless concentration of hydrogen
D	dispersion coefficient $\frac{cm^2}{s}$
d_e	equivalent diameter, cm
F	Faraday's constant
I	total current, A
J	current density, $\frac{mA}{cm^2}$
k	reaction rate constant, appropriate units
L	length, cm
M	number of moles
$N = \frac{D}{UL}$	dispersion number
n	order of reaction
n_e	number of electrons transferred
$-r$	rate of reaction based on volume of fluid, moles of reactant reacted/cm^3 s
S_e	surface of electrode, cm^2
T	absolute temperature, °K
$\bar{t} = \int_0^\infty tE(t)\,dt$	mean residence time, s
U	velocity component in Z direction, $\frac{cm}{s}$
$u = \frac{U}{U_0}$	dimensionless velocity
V_a	volume of system, cm^3
V	operating voltage, V
v	volumetric flow rate, cm^2/s
$x = \frac{M_0 - M}{M_0}$	fractional conversion, degree of conversion of hydrogen
y	mole fraction of hydrogen
Z	space coordinate, cm
$z = \frac{Z}{L}$	fractional length

Greek letters

$\varepsilon = \frac{V_{x=1} - V_{x=0}}{V_{x=0}}$	coefficient of expansion
ρ_m	molar density of fuel, $\frac{\text{g mole}}{cm^3}$
η	overvoltage, V
$\sigma_t^2 = \int_0^\infty (t-\bar{t})^2 E(t)\,dt$	dimensional variance, s^2
σ^2	dimensionless variance
$\tau = \frac{V_a}{v_0}$	space time, s

References

[1] B. S. Baker, Ed., 'Hydrocarbon Fuel Cell Technology', Academic Press, New York (1965).

[2] E. Baur, W. D. Treadwell, and G. Trumpler, *Z. Elektrochem.*, **27** (1921) 199.

[3] C. Berger, 'Handbook of Fuel Cell Technology', Prentice Hall, Englewood Cliffs, N. J. (1968).

[4] J. O'M. Bockris, and S. Srinivasan, 'Fuel Cells: Their Electrochemistry', McGraw-Hill, New York (1969).

[5] M. W. Breiter, 'Electrochemical Processes in Fuel Cells', Springer-Verlag, New York (1969).

[6] G. H. J. Broers, and J. A. A. Ketelaar, 'Fuel Cells', G. J. Young, ed., Reinhold, New York (1960).

[7] G. H. J. Broers, and M. Schenke, *ibid.*

[8] H. H. Chambers and A. D. S. Tantram, *ibid.*

[9] P. V. Danckwerts, *Chem. Eng. Sci.*, **2** (1953) 1.

[10] O. K. Davytan, *Bull. Acad. Sci. U.S.S.R. dasse Sci. Tech.*, **107** (1946) 125.

[11] M. Dudukovič, MS Thesis, Illinois Institute of Technology, Chicago (1970).

[12] L. T. Fan, and R. C. Bailie., *Chem. Eng. Sci.*, **13** (1960) 63,

[13] D. Gidaspow, *A.I.Ch. E. J.*, **13** (1967) 4.

[14] Institute of Gas Technology, 'JP-4 Fueled Molten Carbonate Fuel Cells,' Contract No. *DA-44-009-AMC-1465* (T) for U.S. Army Mobility Equip-

ment Research and Development Center, Fort Belvoir, Virginia (January 1968).
[15] O. Levenspiel, 'Chemical Reaction Engineering', John Wiley, New York (1962).
[16] O. Levenspiel, and K. B. Bischoff, 'Patterns of Flow in Chemical Process Vessels', in 'Advances in Chemical Engineering', Vol. 4, Academic Press, New York (1963).
[17] H. A. Liebhafsky atd E. J. Cairns, 'Fuel Cells and Batteries', John Wiley, New York (1968).
[18] R. W. Lyczkowski, D. Gidaspow, and C. W. Solbrig, *Chem. Eng. Progr. Symp. Ser.*, **63**, No.77 (1967).
[19] S. J. Oleksy, H. Weinstein, and A. B. Shaffer, *J. Appl. Physiol.*, **26** (1969) 227.
[20] R. K. Olson, MS Thesis, Illinois Institute of Technology, Chicago (1967).
[21] A.D.S. Tantram, A. C. C. Tseung, and B. S. Harris, 'Hydrocarbon Fuel Cell Technology', B. S. Baker, ed., Academic Press, New York (1965).
[22] Laan Van der, *Chem. Eng. Sci.*, **7**, (1958) 187.
[23] J. F. Wehner, and R. H. W. Chelen, *Chem. Eng. Sci.*, **6** (1965) 89.
[24] K. R. Williams, 'An Introduction to Fuel Cells', Elsevier, Amsterdam (1966).